

LETTER • OPEN ACCESS

Development of a compact x-ray laser in the ‘water window’ at 4.0 nm

To cite this article: S Suckewer *et al* 2021 *Laser Phys. Lett.* **18** 115001

View the [article online](#) for updates and enhancements.

You may also like

- [Self-channelled high harmonic generation of water window soft x-rays](#)
V Cardin, B E Schmidt, N Thiré *et al.*

- [Attosecond light sources in the water window](#)
Xiaoming Ren, Jie Li, Yanchun Yin *et al.*

- [Effect of fast electrons on emission properties of non-equilibrium nitrogen plasma in soft x-ray spectral range](#)
Vassily S Zakharov and Sergey V Zakharov



IOP | ebooks™

Bringing together innovative digital publishing with leading authors from the global scientific community.

Start exploring the collection—download the first chapter of every title for free.

Letter

Development of a compact x-ray laser in the ‘water window’ at 4.0 nm

S Suckewer^{1,*}, A Morozov¹, A Goltsov^{2,3}, A V Sokolov^{2,3} and M O Scully^{1,2,3}

¹ Princeton University, Princeton, NJ 08544, United States of America

² Texas A&M University, College Station, TX 77843-4242, United States of America

³ Baylor University, Waco, TX 76798, United States of America

E-mail: suckewer@princeton.edu

Received 8 March 2021

Accepted for publication 13 September 2021

Published 7 October 2021



Abstract

A narrow spectral range between 2.3 nm and 4.4 nm wavelengths, the so-called ‘water window’ (WW), provides a unique opportunity for time-resolved imaging of proteins in their natural environment, as water is semi-transparent, while carbon is mostly opaque at these wavelengths. In this work we are presenting experimental developments toward high laser gain in CV ions at 4.03 nm, in a table-top device, and discuss possible application of such an x-ray laser to high-resolution microscopy, as well as generation of attosecond pulses.

Keywords: x-ray laser, water window, ultrafast optics, strong-field physics

(Some figures may appear in colour only in the online journal)

1. Introduction

Over the past half century a significant number of x-ray laser (XRL) schemes have been proposed and analyzed involving, for example: inner shell excitation [1, 2], charge exchange [3], collision excitation [4, 5], ionization and very fast recombination [6], lasing without inversion [7–9], and x-ray Free Electron Laser (X-FEL) [10–12]. High pulse energy of the X-FEL, and wavelength scannable from 0.15 nm through the ‘water window’ (2.3–4.4 nm) and longer wavelengths, make it a very versatile system. Thereby, despite the very large size (\sim km in length), huge cost to build (\sim 1.6 B\$) and to operate (many M\$ yr^{-1}), the X-FEL yields results that justify building such a large-scale expensive instrument [12].

In the meantime, several of the compact XRL schemes have been already experimentally realized. For example, XRLs

have been demonstrated using: collisional excitation schemes [13, 14] as well as recombination schemes [15–18], in which ionization is followed by very fast recombination. Achieving gain using the recombination scheme is highly desirable in the pursuit of XRLs due to requiring relatively low pumping pulse energy. This, combined with the high quantum efficiency achieved by using the transition to the ground state, makes the creation of a practical tabletop XRL in the WW a very attractive goal. Moreover, due to the robustness of the XRL it can be used also by graduate students, especially for experiments with live organisms in water, while access to the X-FEL is very restricted.

Here we present high gain x-ray amplification results in He-like CV ions in comparison with H-like LiIII ions; both are based on a rapid-recombination plasma [6, 15–17]. For this earlier laser action involving the transition to a ground state the powerful sub-picosecond pumping (PSP) KrF laser was operated at a pulse intensity of $\sim 3 \times 10^{17} \text{ W cm}^{-2}$, which is close to the intensity necessary for high gain generation in LiIII (for $n = 2$ to $n = 1$ transitions). The plasma was created by irradiation of a LiF microcapillary with 0.1 J, Nd-glass laser or by irradiation of a LiF slab with a 1 J, 12 nsec Nd-glass laser [16]. The lasers were focused on the entrance of a microcapillary or

* Author to whom any correspondence should be addressed.



Original Content from this work may be used under the terms of the [Creative Commons Attribution 3.0 licence](#). Any further distribution of this work must maintain attribution to the author(s) and the title of the work, journal citation and DOI.

on a slab with various line-focus lengths. Measuring intensity vs. length, for the LiIII(2→1) emission, yielded the gain value.

However, generating XRL pulses at CV 4.03 nm (i.e. in the ‘water window’) requires two orders of magnitude higher pumping intensities than for LiIII, and one order of magnitude higher plasma densities. Reaching such conditions for high gain is a difficult task. It turns out that an even more difficult task is to create a sufficiently long and reasonably uniform plasma waveguide (‘plasma channel’) to obtain the necessary gain-length product $GL \geq 12$ for the XRL pulses to approach the saturated regime of amplification.

In order to increase the length of the high gain region, we have developed a technique for creating the plasma channel, making propagation of ultra-intense and ultra-short pulses with relatively high pulse energy transmission possible. Here we report our results on the channeling in CV at 4.03 nm in comparison with our results on using channeling for the development of a 13.5 nm laser in H-like LiIII ions [6, 15–18].

Aside from the quest for ever shorter wavelength lasers, a major motivation for the present work is developing an XRL as the source of radiation for high resolution x-ray microscopy, allowing us to obtain images of live cells in their natural environment.

In the next section we explain the physics behind the He-like CV XRL at 4.03 nm and present our experimental data. In sections that follow, we discuss extensions of the laser scheme as well as its application to the study of living cells and possibility to generate attosecond pulses.

2. The experimental set up for the CV (2¹P—1¹S) transition laser

XRL schemes based on transitions to the ground state (here $n = 2$ to $n = 1$ transitions), characterized by short lasing wavelength and high quantum efficiency, are particularly attractive. For these schemes the WW lasing is attainable for CV and CVI ions using pump lasers with relatively low energy but high intensity, allowing high repetition rates. Our computer simulations have shown the feasibility of achieving high gain with the transient recombination scheme with peak pump intensity of $2 \times 10^{18} \text{ W cm}^{-2}$ and pulse duration $\sim 100 \text{ fsec}$ for He-like CV ions and of $6 \times 10^{18} \text{ W cm}^{-2}$ for H-like CVI ions [19] in the experimental setup illustrated in figure 1.

Electrons in the high-energy tail of the distribution function, due to their small electron-ion interaction cross section, quickly escape the narrow plasma channel without participating in the recombination processes. After a short time, on the order of a few psec, the bulk of the electrons in the plasma channel ‘decay’ to a Maxwellian electron distribution in about 15–20 psec with a peak energy at about 250–300 eV. Such electron energies are too high for effective three-body recombination process. Therefore, very short and intense laser pulses are required in order to create a high density plasma with fully ionized carbon ions with a highly non-Maxwellian electron energy distribution. The optical field ionization (OFI) processes such as tunneling and multiphoton ionizations are

capable of providing suitable conditions for generating a gain in H-like ions [2, 6, 19].

In the case of transition to the ground state ($n = 1$) from the excited state ($n = 2$) in CVI at 3.374 nm the amplification should occur in an exceptionally short time due to rapid population of the $n = 1$ state. Such rapid population of the CVI ground level in a high density plasma would lead to rapid 3-body recombination of ground state of CVI to highly excited states of CV ions, creating population inversion during the still non-Maxwellian electron energy distribution, leading to the gain generation in the 2→1 transition of singlet CV at 4.03 nm.

Electron densities have to be high (ranging from 10^{17} to 10^{20} cm^{-3} depending on the atomic number Z) and require ultra-short ionizing pulses of high intensity in order to create a population inversion between excited states and the ground state.

The OFI, due to short pumping pulses, does not create significant plasma heating. The main source of plasma heating during the OFI process is above-threshold ionization (ATI) heating. This heating arises from the variation in the oscillation phase between the free electrons (resulting from the ionization of atoms and ions) and the phase of the laser electric field. The average residual energy is proportional to the cycle-averaged quiver energy of the free electrons in the laser field $Eq = (e E \lambda / 2\pi m_e)^2$, where e is the electron charge, E is the laser peak electric field, m_e is the electron mass, c is the speed of light, and λ is the wavelength of the pump laser beam.

Because three-body recombination rates are proportional to the square of the electron density, N_e^2 , and the main quantum number n to power 4, n^4 , the transitions from fully ionized carbon C⁶⁺ to H-like CVI (C⁵⁺) occur primarily to the states with high n , while collisional and radiative transitions to level $n = 2$ are faster than to ground level $n = 1$. This creates a population inversion between excited states with $n \geq 2$ and ground state, $n = 1$. Currently, we are interested primarily in the transition between $n = 2$ and $n = 1$.

In order to minimize plasma heating, the pump pulses have to be ultrashort due to the exceptionally short radiative lifetime τ of the first excited levels of higher Z ions, since τ decreases as $1/Z^4$, where Z is the atomic number of the ions, has to be shorter than the radiative decay time and the collisional decay time at high N_e . Computer simulation has shown that the gain can be enhanced and also become less stringently dependent on exactly matching the required experimental parameters if hydrogen gas is added into the carbon plasma, as the ionization potential of hydrogen is much lower than highly ionized carbon ions. Therefore, introducing free electrons into the plasma by ionization of hydrogen atoms is an efficient process to increase rate of 3-body recombination of C⁵⁺ to C⁴⁺ and C⁴⁺ to C³⁺ hence to increase gains for CVI and CV ions.

Although the experiment in LiIII has shown good promise for our approach for the development of the XRL operating in the WW, the computer modeling for the case of higher Z ions (in particular CVI) indicates a need not only for a pump laser pulse intensity 100 times higher than that used for the LiIII ions but also for a much higher plasma density. Achieving such conditions has proven a difficult task.

Experimental setup

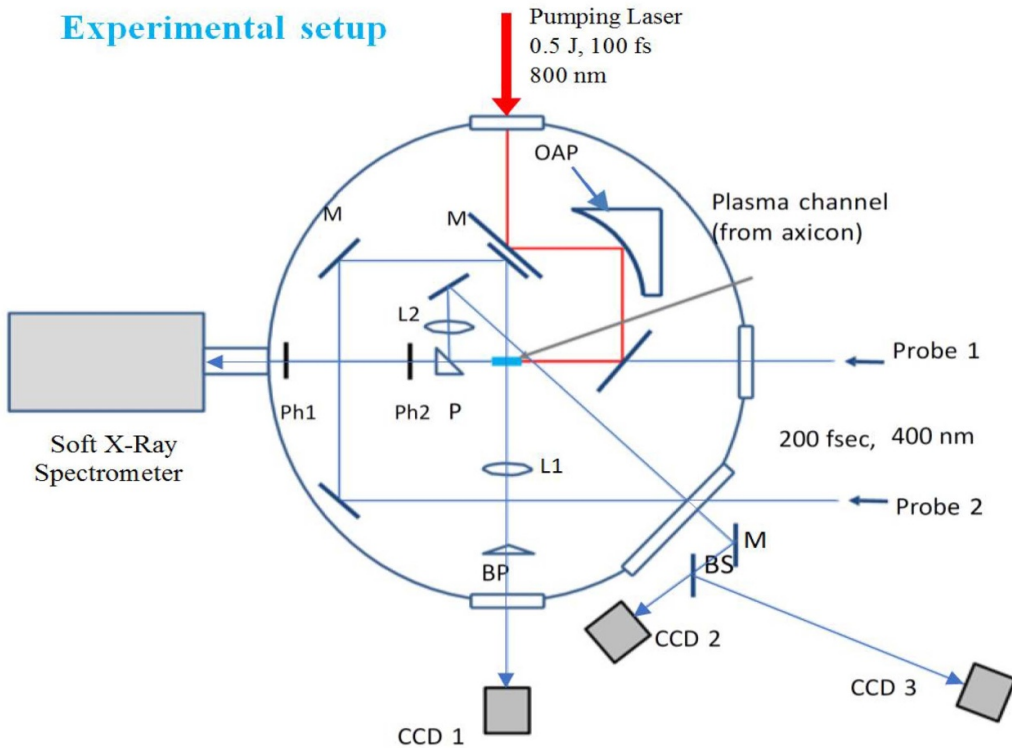


Figure 1. Schematic of the low pressure chamber where the ultraintense fsec IR laser pulses are propagating and generating XRL gain. The target gas jet, produced by a 1 mm nozzle, is located in the very center. The plasma channel is created using an off-axis parabolic mirror (OAP), pinholes (Ph1, Ph2), mirrors (M), lenses (L1, L2) and diagnostics for monitoring reproducibility and quality of plasma channel include: x-ray spectrometer, CCD detectors (CCD1, CCD2, CCD3), prism (P), beam polarizer (BP) and beam splitter (BS).

Namely, the main technical difficulty is in creating a longer plasma channel (a waveguide for the propagation of the high intensity femtosecond pulses of pump laser) without a substantial decrease of the gain along the direction of the pulse propagation.

Initially, to prove experimentally the concept of generating high gain in H-like ions in transitions to the ground states, we conducted an experiment with LiIII (Li^{2+}) ions [15]. It was easier to conduct such an experiment because it requires much lower pump laser intensity than in the case of CVI ions. The experiment demonstrated high gain in the LiIII($2\rightarrow 1$) transition at 13.5 nm and large intensity amplification.

While optimizing plasma and pumping laser parameters to obtain an intense CVI spectrum in the WW and to achieve population inversion for the required transitions, we also found that CVI lines have high intensity, especially for the singlet 2p-1s transition at 4.03 nm.

3. The experimental results

Figure 2 shows the CV and CVI spectra in the wavelength range of 2.8–4.1 nm within the WW. The spectra are measured in the 2nd diffraction order, to obtain higher resolution. The spectra were obtained using a grazing incidence flat-field spectrometer having a diffraction grating of $1200 \text{ grooves mm}^{-1}$ and equipped with a $1024 \times 1024 \text{ CCD}$

camera. In most of our experiments, we used pulse intensities of $(1\text{--}2) \times 10^{18} \text{ W cm}^{-2}$. The plasma was created in short pulses of jet gas mixture consisting of 20% C_2H_6 and 80% H_2 . The neutral gas density and the plasma density above the jet's nozzle slit were simultaneously monitored during these experiments.

Of special interest is the comparison of the two CV spectra in figure 2: one spectrum is obtained in plasma with 'channeling' (part (d)), and the other spectrum is acquired without 'channeling' (part (c)).

The 'plasma channel', which is the plasma waveguide, has to be sufficiently long and uniform in order to enable the delivery of ultra-intense laser pulses to the x-ray lasing region. For example, generating high gain in He-like CV at 4.03 nm requires two orders of magnitude higher pumping intensities than for LiIII, and one order of magnitude higher plasma densities [6, 7]. Achieving such conditions experimentally was a rather difficult task, especially since our goal was to use a low laser energy to build a compact system, which implied producing a very small waveguide diameter. For example, the plasma waveguide FWHM diameter in figure 2(d) was $7 \mu\text{m}$ in order to reach single pulse intensity of $1 \times 10^{18} \text{ W cm}^{-2}$ in $\sim 0.5 \text{ mm}$ long channel for 150 mJ, 100 fsec pumping laser pulses. We attribute the experimentally observed gain and lasing, at peak intensities somewhat below the ones used in our simulations, to the improved 'channeling'.

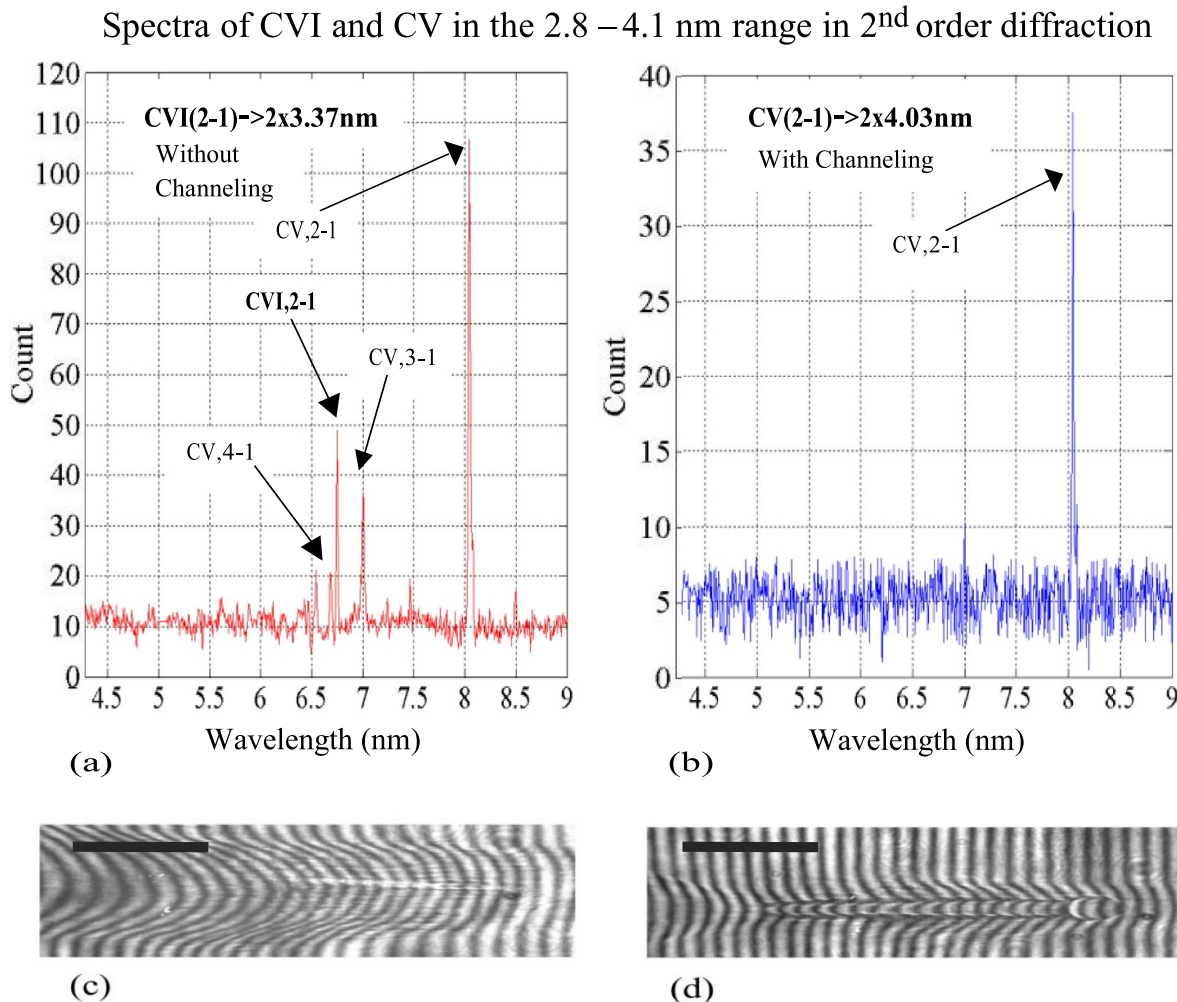


Figure 2. Spectra of CVI and CV in the 2.8–4.1 nm range, in 2nd order diffraction: (a) carbon spectrum obtained with fsec beam of $2 \times 10^{18} \text{ W cm}^{-2}$ peak intensity without plasma channel. The pulse energy was 150 mJ, the gas jet mixture was 20% of C_2H_6 and 80% of H_2 at pressure of 14 psi above surrounding atmospheric pressure ($\sim 1 \text{ atm}$) and at room temperature ($\sim 68 \text{ F}$), which were the same for presented measurements here. (b) Carbon spectrum obtained with plasma channel using $1/2$ of peak intensity of fsec beam ($1 \times 10^{18} \text{ W cm}^{-2}$) in $\sim 0.5 \text{ mm}$ long plasma channel; energies of channeling and fsec pulses were 150 mJ each. The lower beam intensity was sufficient in the case of the pre-formed plasma channel. The initial channel width, and the smallest laser spot size (FWHM), were both measured at $\sim 7 \mu\text{m}$. (c) Interferogram of the plasma (without channeling), in which 100 fsec, 150 mJ laser pulses have been propagated. (d) Interferogram of the plasma (with channeling), in which 100 fsec, 150 mJ laser pulses have been propagated. The preformed plasma channel was created by axicon line focus of 200 psec, 150 mJ laser pulses. The delay time between fsec and psec pulses was 1.2 nsec, the gas jet mixture and its pressure were the same as in other measurements. Scale bars correspond to 0.2 mm length in (c) and (d).

The interferogram of the plasma created by a single high-intensity 100 fsec, 150 mJ pulse was taken immediately after the pulse passed through the jet. The second interferogram was obtained for plasma created by a similar 100 fsec pulse propagating through a pre-formed plasma region, with an additional 200 psec pre-pulse producing an improved waveguide. The 200 psec pulse also had 150 mJ of energy and arrived at the gas target 1.2 nsec prior to the arrival of the 100 fsec pump pulse. The gas target used in this dataset was the same as in the spectrum without plasma channel. The pre-formed plasma waveguide effectively confined the propagation of the 100 fsec ultraintense pulse, maintaining its high intensity over a distance $L_{\text{eff}} \approx 0.5 \text{ mm}$ and creating a significant effect on the intensity of the CV(2 \rightarrow 1) line as shown in figure 2(b).

The most common method of obtaining gain, which has been used for the LiIII 13.5 nm line [16] is from exponential increase lasing line intensity versus length of channel. But it was not applicable for gain measurements in CV 4.03 nm due to very short plasma channel. The gain in He-like CV has been estimated by two methods, described earlier in [6]. The first method was based on comparison of lasing line intensity at the output of the channel with its intensity without channeling, but with the same laser and plasma parameters (including the plasma depth, as well). For implementation of this technique a line CV(3 \rightarrow 1) has been used as an additional reference line for checking plasma and laser consistency during lasing and non-lasing experiments.

The second method was based on simulations, calculating intensities of singlet CV(2 \rightarrow 1) and CV(3 \rightarrow 1) lines for

experimental laser and plasma parameters and their comparison with simulations for LiIII(2→1) at 13.5 nm and LiIII(3→1) at 11.4 nm. The latter ones were used as benchmarks due to their very good agreement with experimental values. Both methods revealed the presence of gain as high as ~ 40 cm $^{-1}$.

This magnitude of gain is consistent with the computer simulations, although since the plasma conditions in the experiments are not known precisely the computer simulations provide only a gain estimate.

4. Applications of the XRL in the WW to high resolution microscopy of live cells and generation of a train of sub-fsec/attosecond pulses

Very high XRL gain at 4.03 nm opens the path toward applications to high resolution microscopy of living cells in a thin layer of water in the x-ray range between Oxygen and Carbon K α edges of 2.3 nm and 4.4 nm, respectively. This WW is the optimal region for high resolution imaging microscopy of live cells, where contrast is high and resolution is very good. Better resolution is possible to obtain at shorter wavelength, however due to much worse contrast at such wavelength the overall imaging quality would be lower.

Most of what is known about high resolution images for studying the internal structure of cells has been learned through electron microscopy. This knowledge rests on the premise that the procedures necessary to prepare a specimen for the electron microscopy do not significantly influence the structural form and the fine details of the observed high-resolution structures. However, there is doubt about the fidelity of the images of such prepared cells in comparison to the images of the original live cells. Because the cell has to be fixed, stained with heavy metals and sectioned to obtain high-resolution images with the electron microscope, fidelity is quite low despite the high resolution of the microscope.

The x-ray microscopy in the WW offers a new way to look at unaltered cells in their natural state. The absorption edges in the x-ray spectra of naturally occurring cell constituents provide sharp contrast without the addition of heavy metals to the cell as in the case of electron microscopy.

Biologists have long sought to observe the structure and function of living cells at high resolution. The short, nanosecond and sub-nanosecond pulses of soft XRLs in the WW enable imaging of cells that are alive the instant before a flash exposure to soft x-rays. The necessary radiation dose levels make it probable that the cells will not survive the exposure, but exposures of different cells should make it possible to piece together new information about dynamic processes in cells, through a version of pump-probe experiments.

This work began at Princeton by using our first recombination XRL at 18.2 nm, pumped by 300 J CO₂ laser (system 1), followed by the second laser pumped by a significantly smaller, very intense KrF excimer laser (system 2). XRLs pumped by these systems 1 and 2 provided similar images of dehydrated normal and cancer cells [6, 18]. Although at 18.2 nm

laser operation the wavelength was far away from WW, we could already use this setup to obtain high resolution images of dehydrated HeLa cancer and normal cells, with clear distinction between membrane contours of cancer and normal cells. The ultimate goal of the XRL microscopy program is to obtain images of live cells.

In WW XRL microscopy, a thin (100 nm) window separates the x-ray vacuum tube from the biological cells located on the window, and their images are recorded at atmospheric pressure, by sensitive photoresist PMMA (or by a CCD with small pixels used at a later stage of the study). We have demonstrated that the XRL beam has sufficient energy to expose images on the photoresist in a single shot. Images of diatom fragments (the silicified skeleton of planktonic algae) on photoresist indicated that the resolution was 50 nm.

Imaging of cancer and normal cells in their natural environment relies on increasing the XRL pulse energy. Demonstration of high gain at 4.03 nm in He-like CV ions is an important step in this direction. This accomplishment holds promise for a new kind of high resolution x-ray microscopy.

Recently, the TAMU-Princeton-IAPRAS team [20, 21] suggested a technique for generation of a train of sub-fsec and individual attosecond pulses by using an XRL with lasing in H-like CVI ions in transition to the ground state. In this way the pulse duration of the table-top XRLs, which is limited by the population decay time of an excited state and typically exceeds hundreds of femtoseconds, can be shortened to sub-fsec/attosecond duration. Such short x-ray pulses would be desirable for dynamical imaging of the fast processes. This technique of generation sub-fsec/attosecond pulses is based on modulation of the frequency of the inverted transition of the XRL by an IR field via the Stark effect, which results in redistribution of the resonant gain. It should be noted that the recombination XRLs based on hydrogen-like ions (such as CVI) are especially promising for the realization of this technique due to degeneracy of the upper laser level and a large dipole moment of the corresponding 2p-2s transition resulting in its efficient interaction with the IR field and hence a deep modulation of the inverted laser transition. The proximity of the |2p,1s> and |2s,1s> states in He-like CV ions in combination with an even higher value of the transition dipole moment also makes CV ions very promising for generation of subfemtosecond pulses by this technique.

Acknowledgments

We would like to thank Dr Olga Kocharovskaya (Texas A&M University) for stimulating discussions on plasma waveguiding ('channeling') of very high intensity femtosecond laser pulses and the waveguiding effect on creation high gain in recombination XRL systems. We also thank Dr Kocharovskaya for pointing out the possibility of generation attosecond pulses by fast modulation of the upper lasing levels of XRL.

S S is thankful to the National Science Foundation for providing funding, making it possible to conduct

experimental research (NSF Grants: 1649047 INSPIRE, 1607613 Development of XRL) and to Princeton University for its overall support.

A S acknowledges support from the Robert A Welch Foundation (Grant No. A-1547).

M S would like to thank the Air Force Office of Scientific Research (Award No. FA9550-18-1-0141), the National Science Foundation (Grant No. 2013771), the Office of Naval Research (Award No. N00014-20-1-2184), the Robert A Welch Foundation (Grant No. A-1261), and the King Abdulaziz City for Science and Technology (KACST) for their support of this work.

Conflict of interest

The authors declare no competing interests.

References

- [1] Duguay M A and Rentzepis P M 1967 Two-photon excitation of fluorescence by picosecond light pulses *Appl. Phys. Lett.* **10** 350
- [2] Keldysh L V 1965 Ionization in the field of a strong electromagnetic wave *Sov. Phys. J. Exp. Theor. Phys.* **20** 1307
- [3] Burnett N H and Corkum P B 1989 Cold-plasma production for recombination extreme-ultraviolet lasers by optical-field-induced ionization *J. Opt. Soc. Am. B* **6** 1195
- [4] Rocca J, Shlyaptsev V, Tomasel F G, Cortázar O D, Hartshorn D and Chilla J L A 1994 Demonstration of a discharge pumped table-top soft-x-ray laser *Phys. Rev. Lett.* **73** 2192
- [5] Attwood D 1999 *Soft X-Rays and Extreme Ultraviolet Radiation: Principles and Applications* (Cambridge: Cambridge University Press)
- [6] Suckewer S and Jaeglé P 2009 X-ray laser: past, present, and future *Laser Phys. Lett.* **6** 411
- [7] Kocharovskaya O and Khanin Y 1988 Coherent amplification of the ultrashort pulse in the three-level medium without population inversion *J. Exp. Theor. Phys. Lett.* **48** 630
- [8] Harris S E 1989 Lasers without inversion: interference of lifetime-broadened resonances *Phys. Rev. Lett.* **62** 1033
- [9] Scully M, Zhu S-Y and Gavrielides A 1989 Degenerate quantum-beat laser: lasing without inversion and inversion without lasing *Phys. Rev. Lett.* **62** 2813
- [10] Pellegrini C et al 1993 A 2–4 nm high power fel on the slac linac *Nucl. Instrum. Methods Phys. Res. A* **331** 223
- [11] Pellegrini C, Marinelli A and Reiche S 2016 The physics of x-ray free-electron lasers *Rev. Mod. Phys.* **88** 015006
- [12] Emma P, Bane K, Cornacchia M, Huang Z, Schlarb H, Stupakov G and Walz D 2004 Femtosecond and sub-femtosecond x-ray pulses from a self-amplified spontaneous-emission-based free-electron laser *Phys. Rev. Lett.* **92** 074801
- [13] Rocca J, Kapteyn H, Attwood D, Murnane M, Menoni C and Anderson E 2006 Tabletop lasers in the extreme ultraviolet *Opt. Photonics News* **17** 30
- [14] Lemoff B, Yin G, Gordon C, Barty C and Harris S E 1995 Demonstration of a 10-Hz femtosecond-pulse-driven XUV laser at 41.8 nm in Xe IX *Phys. Rev. Lett.* **74** 1574
- [15] Suckewer S, Skinner C H, Milchberg H, Keane C and Voorhees D 1985 Amplification of stimulated soft x-ray emission in a confined plasma column *Phys. Rev. Lett.* **55** 1753
- [16] Korobkin D V, Nam C H, Suckewer S and Goltsov A 1996 Demonstration of soft x-ray lasing to ground state in LiIII *Phys. Rev. Lett.* **77** 5206
- [17] Suckewer S, Sokolov A V and Scully M O 2021 Compact X-ray laser amplifier in the ‘water window’ *Spectrochim. Acta A* **255** 119675
- [18] Suckewer S and Skinner C H 1990 Soft x-ray lasers and their applications *Science* **247** 1553
- [19] Avitzour Y and Suckewer S 2007 Feasibility of achieving gain in transition to the ground state of C VI *J. Opt. Soc. Am. B* **24** 819
- [20] Akhmedzhanov T, Antonov V, Morozov A, Goltsov A, Scully M O, Suckewer S and Kocharovskaya O 2017 Formation and amplification of sub-femtosecond x-ray pulses in a plasma medium of the hydrogen-like ions with a modulated resonant transition *Phys. Rev. A* **96** 033825
- [21] Antonov V, Han K C, Akhmedzhanov T, Scully M O and Kocharovskaya O 2019 Attosecond pulse amplification in a plasma-based x-ray laser dressed by an infrared laser field *Phys. Rev. Lett.* **123** 243903